

Cumulative Deformation Capacity of Buckling Restrained Braces Taking Buckling of Core Plates into Account

Ryota Matsui & Toru Takeuchi

Tokyo Institute of Technology, Japan



SUMMARY

Buckling restrained braces (BRBs) are widely used as seismic resistant and seismic energy dissipation devices. As an energy dissipation brace, one key limiting state of BRBs is governed by cumulative deformation capacity up to and until core-plate fracture. Such capacity will always be less than that of the steel material employed. The view expressed in this paper is that the mechanism decreasing cumulative deformation capacity in the BRB is attributable to local buckling of the core plate, which leads to non-uniform strain distribution of the core plate in a longitudinal direction. This decrease in the cumulative deformation capacity of the BRB can be explained by applying the fatigue performance formula for the relevant steel material to the strain encountered at the local zone of the core plate. A ratio that compares degree of strain concentration at this localized zone with the total normalized deformation is proposed as determining the strain at the core plate local zone relative to total normalized deformation. In addition, the effect of the exponential value of the fatigue performance formula on methods for predicting cumulative deformation capacity of the BRB is investigated.

Keywords: Buckling Restrained Brace, Local Buckling, Cumulative Deformation Capacity, Fatigue Fracture

1. INTRODUCTION

Buckling restrained braces (BRBs) are widely used as seismic resistant and energy dissipation devices. As an energy dissipation brace, one key limiting state of BRBs is determined by cumulative deformation capacity until the core plate fractures. The BRB's capacity for stable dissipation of energy when its restraint conditions are satisfied allows for absorption of seismic energy. This absorption eventually leads to fracture of the BRB. Since BRBs are generally designed to avoid fracture during seismic events, determining cumulative capacity for energy dissipation proves crucial in evaluating performance and in assessing any needed replacement.

Several researchers have confirmed that the core plate of the BRB undergoes a high-mode buckling deformation that leads to non-uniform strain distribution. In particular, Takeuchi and Hajjar, et al., (2010) studied such high-mode buckling of the core plate in BRBs.

Cumulative deformation capacity of the BRB itself is most generally evaluated directly, using the Manson–Coffin fatigue formula to resolve fatigue performance in BRBs. However, cumulative deformation capacity should be evaluated initially by applying the fatigue performance formula to the strain concentration zone in the steel material of the core plate itself.

In this paper, the mechanism that decreases cumulative deformation capacity of the BRB— other than steel material specifications— is sought in examination of local buckling of the core plate. This buckling leads to non-uniform strain distribution of the core plate in a longitudinal direction. This, in turn, causes a plastic strain concentration in the localized zone. Decrease in the cumulative deformation capacity of the BRB is accounted for by applying the fatigue performance formula for steel material to the strain at the local zone. A ratio comparing strain concentration degree at the local zone with the total normalized deformation is proposed to differentiate strain at the local zone from the total normalized deformation. Finally, the cumulative deformation capacity of the BRB can be evaluated using the local zone strain already calculated from the total normalized deformation.

In addition, the effect of the exponential value of the fatigue performance formula on the methods for predicting cumulative deformation capacity of the BRB was also investigated.

2. FATIGUE FORMULA FOR BRB

From various past experiments on BRBs, Takeuchi and Ida, et al., (2008) proposed the following low-cycle fatigue formula for the BRB as Eq. (2.1)

$$\Delta\varepsilon_n = 0.5 \cdot N_f^{-0.14} + 54.0 \cdot N_f^{-0.71} \quad (2.1)$$

Here, $\Delta\varepsilon_n$ is the normalized deformation amplitude, and N_f is the fracture cycle number. In addition, the results of Takeuchi and Shirabe, et al., (2006) have been employed in Eq. (2.1) to obtain Eq. (2.2) for a fracture cycle number of less than 20.

$$N_f = \left(1 - \frac{3\Delta\varepsilon_n}{70}\right) \cdot \left(\frac{\Delta\varepsilon_n^{-1.41}}{3.63 \times 10^{-3}}\right) + 0.75 \quad (2.2)$$

This modification expresses a partial concentration of plastic strain in the core plate at ultra-low fatigue failure zones, where stress exceeds maximum value and the tangent modulus becomes negative. The fatigue formula for a BRB derived jointly from Eqs. (2.1/ 2.2) is consistent with results based on the experimental data from Nakamura and Takeuchi, et al., (2000), as shown in Figure 2.1. In this figure, the fatigue performance of the BRB will be less than the fatigue performance of the steel material determined on the basis of the normalized deformation amplitudes given by Eq. (2.3).

$$\begin{cases} \Delta\varepsilon_n = 0.74N_f^{-0.11} + 35.0N_f^{-0.47} & (\text{SS400}) \\ \Delta\varepsilon_n = 0.47N_f^{-0.087} + 33.0N_f^{-0.48} & (\text{LY100}) \\ \Delta\varepsilon_n = 0.88N_f^{-0.14} + 72.0N_f^{-0.55} & (\text{LY225}) \end{cases} \quad (2.3)$$

3. STRAIN CONCENTRATION AT CORE PLATES

Takeuchi and Suzuki, et al., (2006) have proposed an index of strain-concentration-ratio for ordinary circular tube braces, whereby the local strain at the point of plastic strain concentration is divided by the normalized deformation. The strain concentration ratio is defined by individual specification of each brace. This index enables one to estimate local plastic strain without significant calculation, such as arise from use of the finite element method. Brace fracture is then simply defined by the point at which local strain value becomes equivalent to the fatigue formula for the steel material. Therefore,

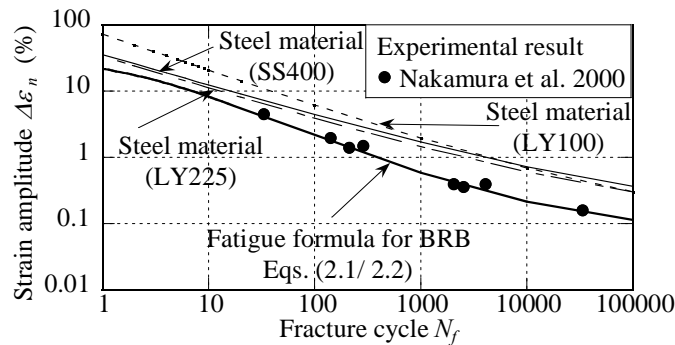


Figure 2.1. Low-cycle fatigue capacity for BRBs and steel material

this method efficiently assesses brace fracture using a macro-model of the braces in question. In this paper, the authors have attempted to evaluate BRB fracture using a similar method.

In our study, the BRB is constituted by a plane steel core plate restrained by a mortar filled steel tube, as shown in Table 3.1. and in Figures 3.1. and 3.2. The mechanical property of SN400 is assumed to be same as that of SS400. Hypothetically, the core plate exhibits a high-mode local buckling deformation continuously within the clearance between the core plate and the restrainer s under cyclic loading. In such case, the local buckling deformation y is calculated from the half amplitude of the local buckling wave l_p as Eq. (3.1).

$$\begin{cases} y = s \sin(\pi x/l_p) \\ s = s_0 + 0.5\nu_p \varepsilon_{eqm} t_c \end{cases} \quad (3.1)$$

Here, ε_{ntm} is the maximum value of normalized tensile deformation, and s_0 is the initial value of the clearance between core plate and restrainer. Although local buckling occurs both in- and out-of-plane, only the latter is considered initially. The half amplitude of the local buckling wave l_p is calculated as Eq. (3.2),

$$l_p = \pi t_c \sqrt{E_t/3\sigma_{cy}}/2 \quad (3.2)$$

where t_c represents thickness of the core plate, σ_{cy} yield stress of the core plate, and E_t the tangent modulus of the steel material. The stress–strain hysteresis curve can be modeled by the modified

Table 3.1. Mechanical Properties of BRB

Specimen	Steel	t_c (mm)	B_c (mm)	$\Delta\varepsilon_n$ (%)	N_f	Input strain amplitude
400-200	SN400B (SS400)	25	100	2	176	Constant (Nakamura et al. 2000)
400-150				1.5	140	
400-040				0.4	211	
100-150	LY100	25	100	1.5	287	
100-040				0.4	2041	
235-150	LY225	28	100	4.5	33	
235-016				0.16	2520	
-	SS400	12	50	3.2	19	Random (Takeuchi et al. 2010)

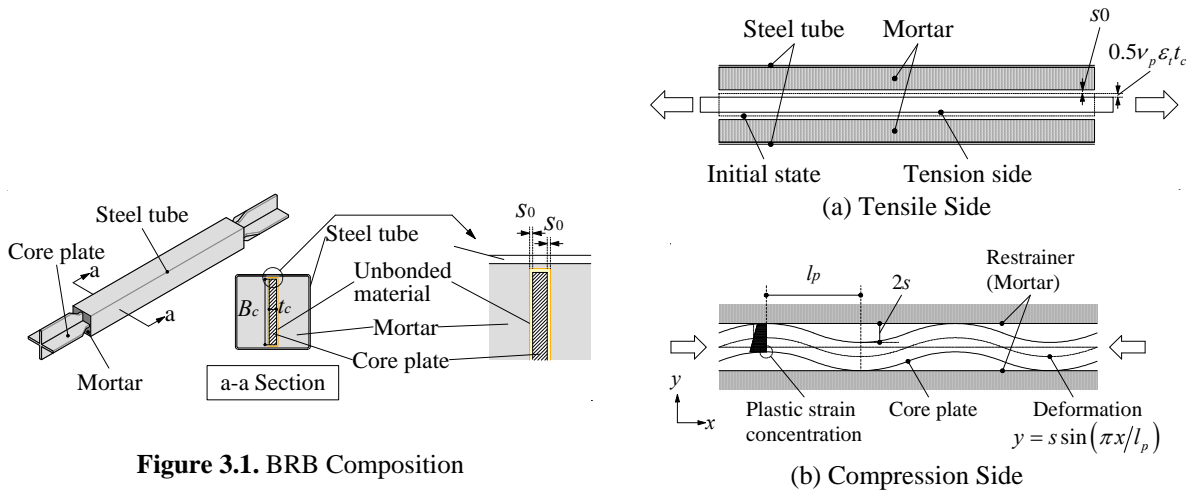


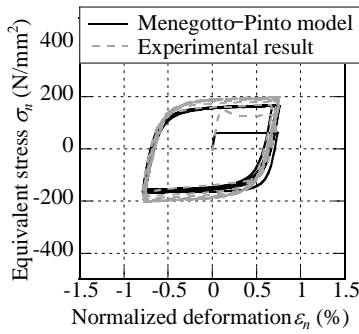
Figure 3.1. BRB Composition

Figure 3.2. Core Plate Deformation

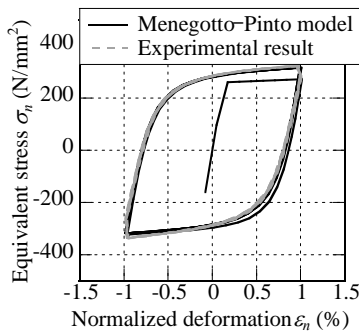
Menegotto–Pinto model, as proposed by Yamazaki and Kasai, et al., (2006). The hysteresis curve calculated using the Menegotto–Pinto model is consistent with the experimental results obtained by Nakamura and Takeuchi, et al., (2000) as demonstrated in Figure 3.3. Here, ε_n is the normalized deformation, while σ_n is the equivalent stress calculated by dividing axial force by initial sectional area. The amplitude of the normalized deformation $\Delta\varepsilon_n$ is defined as Eq. (3.3), as shown in Figure 3.4.

$$\Delta\varepsilon_n = \varepsilon_{nm} - \varepsilon_n \tag{3.3}$$

The tangent modulus E_t is directly calculated using the proposed Menegotto–Pinto model. Here, for ease, the tangent modulus is approximated by the normalized deformation function as Eq. (3.4), illustrated in Figure 3.5.



(a) 100-150 Specimen



(b) 400-200 Specimen

Figure 3.3. Menegotto-Pinto Model

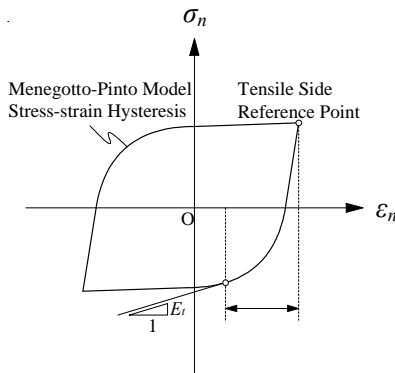
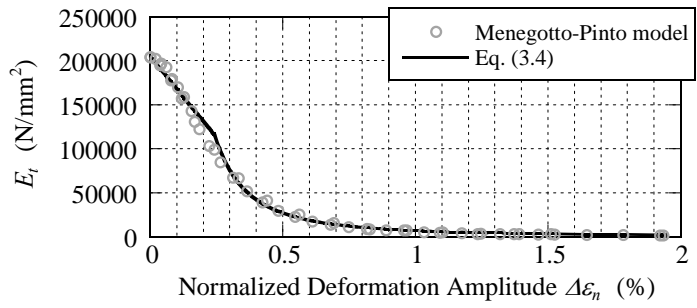
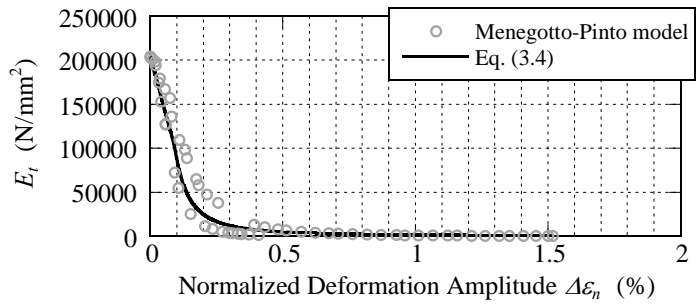


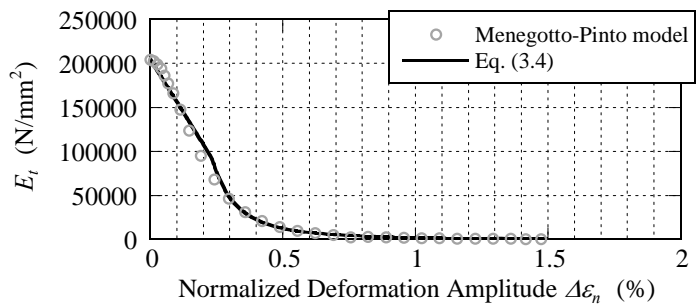
Figure 3.4. Normalized Deformation



(a) SS400



(b) LY100



(c) LY225

Figure 3.5. Tangent modulus of core plate

$$E_t = \begin{cases} \begin{cases} -3.68 \times 10^5 \cdot \Delta \varepsilon_n + E & (\text{SS400}) \\ -1.12 \times 10^5 \cdot \Delta \varepsilon_n + E & (\text{LY100}) \\ -4.84 \times 10^5 \cdot \Delta \varepsilon_n + E & (\text{LY225}) \end{cases} & (0 \leq \Delta \varepsilon_{eq} \leq 2\varepsilon_y) \\ \begin{cases} 6.45 \times 10^3 \cdot \Delta \varepsilon_n^{-2.04} + E & (\text{SS400}) \\ 1.27 \times 10^3 \cdot \Delta \varepsilon_n^{-1.84} + E & (\text{LY100}) \\ 1.93 \times 10^3 \cdot \Delta \varepsilon_n^{-2.65} + E & (\text{LY225}) \end{cases} & (2\varepsilon_y \leq \Delta \varepsilon_{eq}) \end{cases} \quad (3.4)$$

The local buckling deformation gives the bending strain ε_b as in Eq. (3.5).

$$\varepsilon_b = t_c / 2 \left(\pi / l_p \right)^2 s = 6s \sigma_{cy} / E_t t_c \quad (3.5)$$

The geometrical deformation ε_g is additional to the normalized deformation ε_n as in Eq. (3.6).

$$\varepsilon_g = 1/4 \left(\pi s / l_p \right)^2 = 3s^2 \sigma_{cy} / E_t t_c^2 \quad (3.6)$$

The local strain amplitude $\Delta \varepsilon_h$ at the point at which the most concentrated plastic strain occurs in the core plate is calculated using Eq. (3.7), and strain concentration ratio is α_c as defined by Eq. (3.8).

$$\Delta \varepsilon_h = \Delta \varepsilon_n + \varepsilon_b - \varepsilon_g \quad (3.7)$$

$$\alpha_c = \frac{\Delta \varepsilon_h}{\Delta \varepsilon_n} = \frac{\Delta \varepsilon_n + \varepsilon_b - \varepsilon_g}{\Delta \varepsilon_n} \quad (3.8)$$

Local in-plane strain may also be calculated using Eqs. (3.3) ~ (3.7) by substituting the thickness of the core plate t_c for the width of the core plate B_c . The local in-plane strain is generally one eighth (1/8) the local strain out-of-plane. Moreover, maximum strain positions do not necessarily coincide in- and out-of-plane. Therefore, the effect of in-plane local buckling generally does not significantly affect cumulative deformation capacity of a BRB, so that out-of-plane strain is considered as predominant overall.

4. EVALUATION OF CUMULATIVE DEFORMATION CAPACITY

A BRB fracture can be established as the point at which local strain—calculated from normalized deformation ε_n and multiplied by strain concentration ratio α_c —is consistent with the fatigue formula given in Eq. (2.3). Using this evaluation method, the BRB fatigue formula may be assessed as shown in Figure 4.1. The plots in this figure show experimental results derived from Nakamura and Takeuchi, et al., (2000) and Takeuchi and Ohyama, et al., (2010). This fatigue formula is by and large consistent with experimental results. Here, strain amplitude derived from experimental results using random amplitudes is assessed by the rain-flow method as the average plastic strain amplitude, and cumulative plastic strain is the sum of all plastic strains. The initial clearance between the core plate and the restrainer s_0 is set at 1 mm in Nakamura and Takeuchi, et al., (2000) and at 2 mm in Takeuchi and Ohyama, et al., (2010). Figure 4.1. demonstrates that performance given by the BRB fatigue formula decreases as the clearance s between core plate and restrainer increases. Therefore, the strain-concentration-ratio α_c of a BRB may be described as a function of clearance s . For example, the strain-concentration-ratio α_c is approximated as in Eqs. (4.1/ 4.2) by the least squares method, as shown in Figure 4.2., where ε_y is the yield strain and $\Delta \varepsilon_n$ the strain amplitude, when the fracture cycle number is 20.

$$\alpha_c = \frac{\Delta \varepsilon_h}{\Delta \varepsilon_n} = \begin{cases} 1 & (\Delta \varepsilon_n \leq 2\varepsilon_y) \\ 1 + 25 \frac{s}{t_c} f(\Delta \varepsilon_n) & (2\varepsilon_y \leq \Delta \varepsilon_n \leq \Delta \varepsilon_{low}) \\ 1 + 25 \frac{s}{t_c} \beta & (\Delta \varepsilon_{low} \leq \Delta \varepsilon_n) \end{cases} \quad (4.1)$$

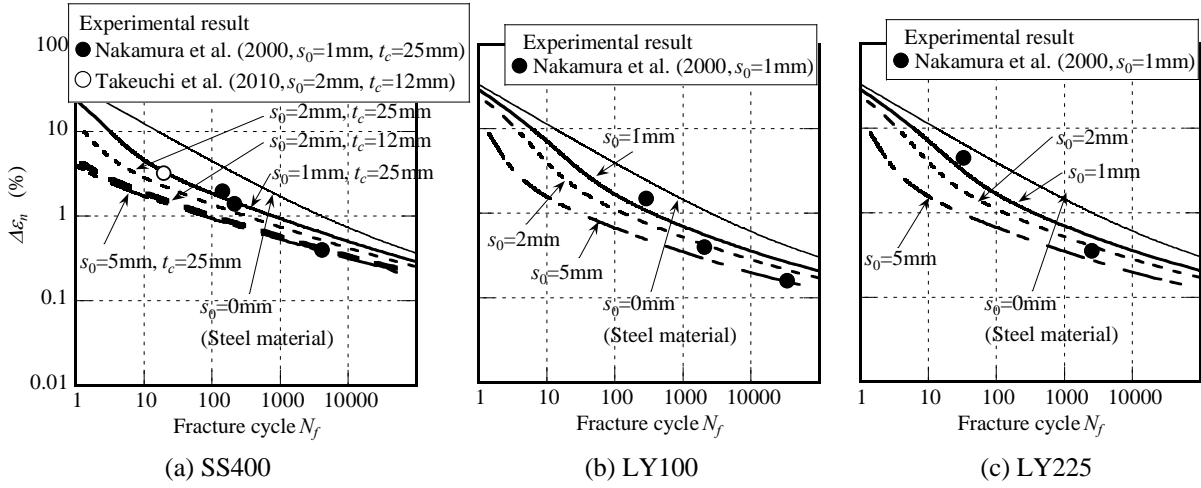


Figure 4.1. BRB Fatigue Formulas Based on Eqs. (3.7/ 3.8)

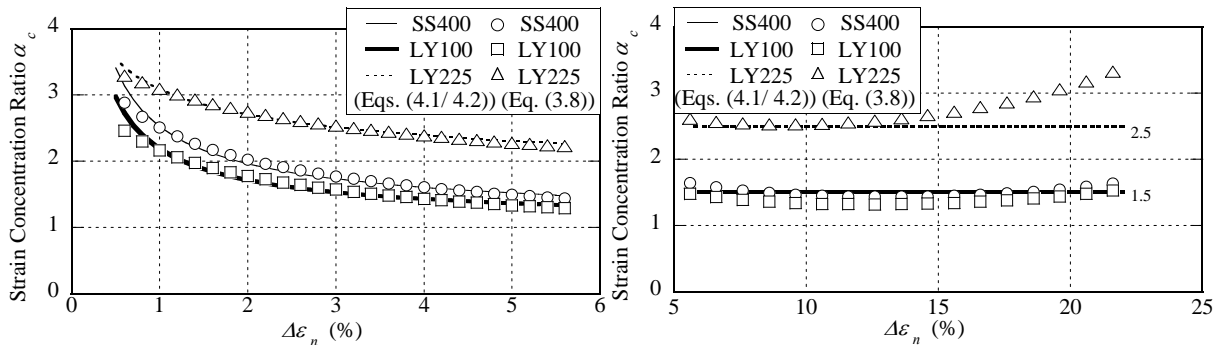


Figure 4.2. Strain Coefficient Ratio

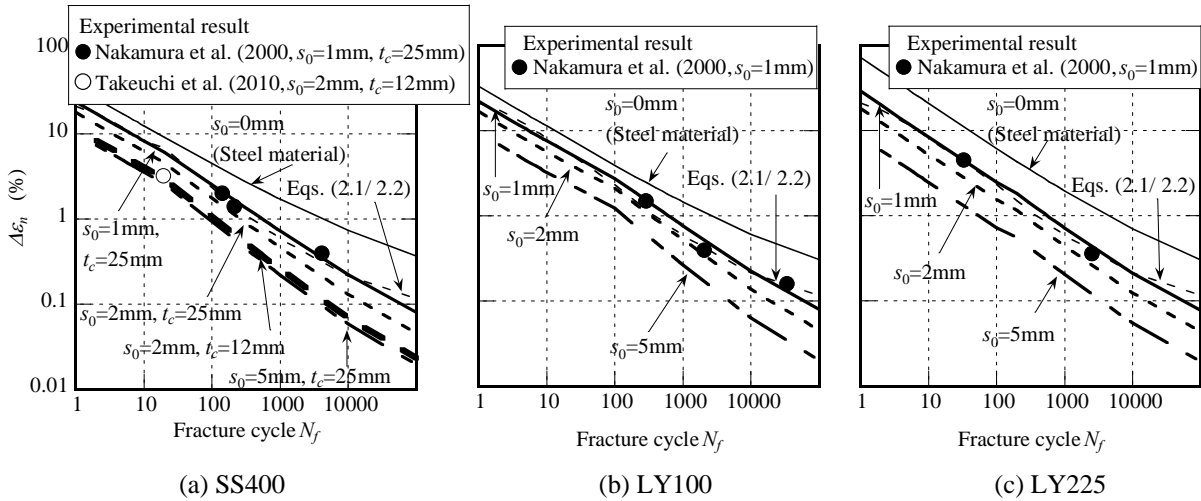


Figure 4.3. BRB Fatigue Formulae based on Eqs. (4.1/ 4.2)

$$\left\{ \begin{array}{l} f(\Delta\varepsilon_n) = \begin{cases} 1.90\Delta\varepsilon_n^{-0.62} & (\text{SS400}) \\ 1.51\Delta\varepsilon_n^{-0.64} & (\text{LY100}) \\ 2.82\Delta\varepsilon_n^{-0.35} & (\text{LY225}) \end{cases} \\ \beta = \begin{cases} 0.5 & (\text{SS400}) \\ 0.5 & (\text{LY100}) \\ 1.5 & (\text{LY225}) \end{cases} \end{array} \right. \quad (4.2)$$

In Figure 4.3., Eqs. (4.1/ 4.2) are compared with behaviour of restrainers, which is generally consistent with our test results.

5. DAMAGE FACTOR EVALUATION BY AVERAGE PLASTIC STRAIN AMPLITUDE

The fatigue evaluation of BRBs was originally based on constant stress amplitudes. Conversely, the amplitude of the response of each member subjected to seismic input is random. In such a case, stress amplitude distribution is generally determined by the rain-flow method.

As an approach to applying the fatigue formula under random amplitude, as in Eq. (2.3), Miner (1945) defined a fatigue condition based on Eq. (5.1). Here, as soon as the cumulative damage factor of individual amplitude reaches 1.0, the element is considered as exhibiting fatigue failure.

$$D = \sum_{i=1}^m D_i = \sum_{i=1}^m \frac{n_i}{N_{fi}} \quad (5.1)$$

Here, D is the damage factor, n_i the number of cycles for the strain amplitude, and N_{fi} the number of failure cycles for a given strain amplitude. Additionally, Takeuchi and Ida, et al., (2008) proposed a method whereby average plastic strain amplitude is applied to fatigue failure conditions, as performed in evaluation in the previous section. In this section, the difference between Miner's rule and average plastic strain amplitude is discussed. The number of fracture cycles is defined for average plastic strain amplitude by Eq. (5.2).

$$\overline{N}_f = \left(\frac{\overline{\Delta\varepsilon_p}}{C_2} \right)^{-\frac{1}{m_2}} \quad (5.2)$$

Here, $\overline{\Delta\varepsilon_p}$ is the average plastic strain amplitude, and C_2 and m_2 are exponential values of the fatigue formula within the range of the plastic region. Cumulative plastic strain is calculated as in Eq. (5.3).

$$\sum \overline{\Delta\varepsilon_p} = 2 \cdot \overline{N}_f \cdot \overline{\Delta\varepsilon_p} = \frac{2 \cdot \overline{\Delta\varepsilon_p}^{\frac{m_2-1}{m_2}}}{C_2^{-m_2}} \quad (5.3)$$

Conversely, cumulative plastic strain calculation by applying Miner's rule is shown as Eq. (5.4)

$$\left\{ \begin{array}{l} \sum \overline{\Delta\varepsilon_p} = 2 \sum_{i=1}^m n_i \Delta\varepsilon_p \\ \sum_{i=1}^m \frac{n_i}{N_{fi}} = 1 \end{array} \right. \quad (5.4)$$

When the exponential value $m_2 = 1.0$, Eq. (5.3) will be identical to Eq. (5.4), with both evaluations perfectly consistent. Thus, the difference between evaluations must rely on the exponential value m_2 . To investigate the influence of the exponential value m_2 , seismic response analysis results obtained by Takeuchi and Miyazaki (2006) were used. The analysis model was a 15-story, rigid BRB frame. For seismic-wave input, BCJ-L2, El Centro NS, Hachinohe EW, Taft EW, and JMA Kobe NS were applied. Maximum velocities for these seismic wave inputs were normalized at 75 cm/s. The ratio of the stiffness of the frame to that of the BRB was 1.0. BRB core plate material was LY225. Figure 5.1. displays damage factors calculated using Miner's rule with average plastic strain amplitude; Figure 5.2. shows their ratios, indicating that damage factors increase as the exponential value m_2 decreases from 1.0. From Eq. (2.1) we see the exponential value m_2 is 0.71, and the damage factor calculated using Miner's rule is approximately 1.2 times that calculated using average plastic strain amplitude. Takeuchi and Ida (2008) reported that the damage factor calculated using average plastic strain amplitude affords a degree of accuracy better than that calculated by Miner's rule— and easier to evaluate, as it does not require individual amplitudes. To obtain the results of this study, the present authors have taken average plastic strain amplitude as an index for evaluating cumulative deformation capacities of BRBs under the strain of random amplitudes in preference to applying Miner's method.

6. CONCLUSIONS

In this paper, the cumulative deformation capacity of BRBs is assessed using steel materials and mechanical models. In addition, evaluation of damage factors regarding such material under random amplitudes through seismic response analysis is discussed. Conclusions are here summarized in the following three statements:

- 1) Strain-concentration-ratios of BRBs are attributed to a mechanism that reveals high-mode local

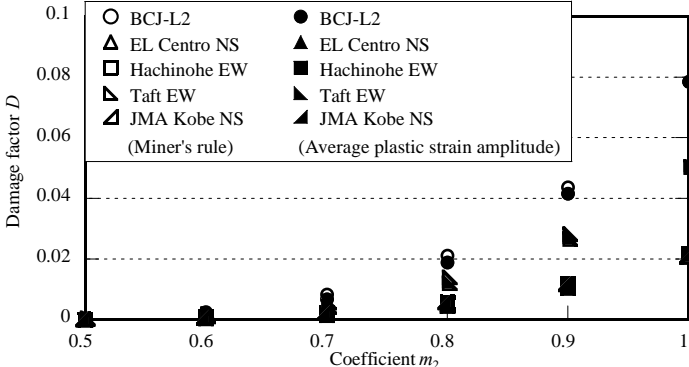


Figure 5.1. Differences in Evaluation by Miner's Rule Evaluation Using Average Plastic Strain Amplitude

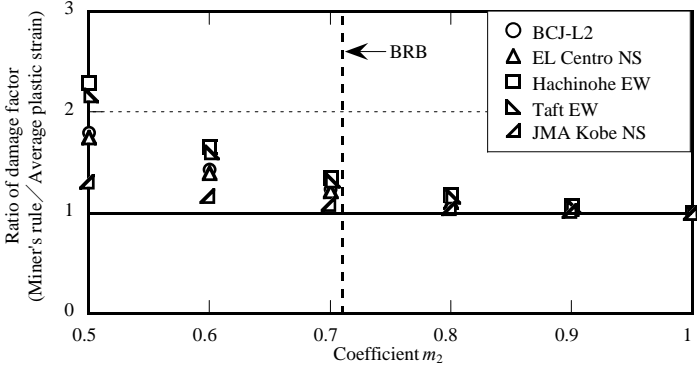


Figure 5.2. Ratio of Damage Factor

- buckling as it occurs in the clearance between core plate and restrainer.
- 2) The fatigue formula for a BRB evaluated from strain-concentration-ratio shows this clearance affecting the cumulative deformation capacity of a BRB, which in turn explains the test results.
 - 3) The damage factors for steel materials calculated by Miner's rule slightly increases from those calculated using average plastic strain amplitude, as the exponential value of the fatigue formula decreases from 1.0.

REFERENCES

- Miner, M. A. 1945. Cumulative Damage in Fatigue, *Journal of Applied Mechanics*, **Vol. 12**, A159-A164
- Saeki, E., Sugisawa, M., Yamaguchi, T., Mochizuki, H., and Wada, A. 1995. A Study on Low Cycle Fatigue Characteristics of Low Yield Strength Steel, *Journal of Structural and Constructional Engineering*, Architectural Institute of Japan, **No. 472**, 139-147 (in Japanese)
- Shimokawa, H., Morino, S., Kamiya, M., Ito, S., Kawaguchi, J., Kamura, H. and Hirota, M. 1998. Elasto Plastic Behavior of Flat-Bar Brace Stiffened by Square Steel Tube (Part 7), Summaries of technical papers of the Annual Meeting of the Architectural Institute of Japan. **C-1, Structures III**, "Timber structures, steel structures, and steel reinforced concrete structures", 843-844, (in Japanese)
- Nakamura, H., Takeuchi, T., Maeda, Y., Nakata, Y., Sasaki, T., Iwata, M., and Wada, A. 2000. Fatigue Properties of Practical Scale Unbonded Braces, *Nippon Steel Technical Report*, Nippon Steel Corporation, **No. 82**, 51-57
- Takeuchi, T., Shirabe, H., Yamada, S., Kishiki, S., Suzuki, K., Saeki, E., and Wada, A. 2006. Cumulative Deformation Capacity and Damage Evaluation for Elasto-plastic Dampers at Beam Ends, *Journal of Structural and Constructional Engineering*, Architectural Institute of Japan, **No. 600**, 115-122 (in Japanese)
- Takeuchi, T. and Miyazaki, K. 2006. Estimation of Cumulative Deformation Capacity for Buckling Restrained Braces Placed in Frames, *Journal of Structural and Constructional Engineering*, Architectural Institute of Japan, **No. 603**, 155-162 (in Japanese)
- Yamazaki, H., Kasai, K., Ono, Y., Kaneko, H., and Sadasue, K. 2006. Curved Hysteresis Model of Structural Steel under Cyclic Loading (Part 3), Summaries of technical papers of the Annual Meeting Architectural Institute of Japan. **C-1, Structures III**, "Timber structures, steel structures, steel reinforced concrete structures", 935-936, Japan (in Japanese)
- Takeuchi, T., Suzuki, K., Matsui, R. and Ogawa, T. 2006. Cumulative Cyclic Deformation Capacity of Tubular Braces with Local Buckling, *Journal of Structural and Constructional Engineering*, Architectural Institute of Japan, **No. 608**, 143-150 (in Japanese)
- Takeuchi, T., Ida, M., Yamada, S., and Suzuki, K. 2008. A. Estimation of Cumulative Deformation Capacity of Buckling Restrained Braces, *Journal of Structural Engineering*, ASCE, **Vol. 134, No. 5**, 822-831
- Koetaka, Y., Kinoshita, T., Inoue, K. and Iitani, K. 2008. Criteria of Buckling-Restrained Braces to Prevent Out-of-Plane Buckling, 14th World Conference on Earthquake Engineering, Paper No. 05-05-0121
- Takeuchi, T., Hajjar, J. F., Matsui, R., Nishimoto, K. and Aiken, I. D. 2010. Local buckling restraint condition for core plate in buckling restrained braces, *Journal of Constructional Steel Research*, Elsevier, **Vol. 66, Issue 2**, 139-149
- Midorikawa, M., Sasaki, D., Asari, T., Murai, M. and Iwata, M. 2010. Experimental Study on Buckling Restrained Braces Using Steel Mortar Planks (Effects of the clearance between core plate and restraining member on compressive strength and estimation of the number of buckling mode related to compressive

strength), Journal of Structural and Constructional Engineering, Architectural Institute of Japan, **Vol. 75, No. 653**, 1361-1368 (in Japanese)

Takeuchi, T., Ohyama, T., and Ishihara, T. 2010. Cumulative Cyclic Deformation Capacity of High Strength Steel Frames with Energy Dissipation Braces (Part 1), Journal of Structural and Constructional Engineering, Architectural Institute of Japan, **Vol. 75, No. 655**, 1671-1679 (in Japanese)